JOC The Journal of Organic Chemistry

Article

pubs.acs.org/joc

Water Encapsulation in a Polyoxapolyaza Macrobicyclic Compound

Pedro Mateus,[†] Rita Delgado,*[,†] Patrick Groves,[†] Sara R. R. Campos,[†] António M. Baptista,[†] Paula Brandão,[‡] and Vítor Félix[§]

[†]Instituto de Tecnologia Química e Biológica, Universidade Nova de Lisboa, Av. da República, 2780-157 Oeiras, Portugal

[‡]Departamento de Química, CICECO, and [§]Secção Autónoma de Ciências da Saúde, Universidade de Aveiro, 3810-193 Aveiro, Portugal

Supporting Information

ABSTRACT: A new heteroditopic macrobicyclic compound ($t_2pN_5O_3$) containing two separate polyoxa and polyaza compartments was synthesized in good yield through a [1 + 1] "tripod−tripod coupling" strategy. The X-ray crystal structure of $H_3t_2pN_5O_3^{3+}$ revealed the presence of one encapsulated water molecule accepting two hydrogen bonds from two protonated secondary amines and donating a hydrogen bond to one amino group. The acid−base behavior of the compound was studied by potentiometry at 298.2 K in aqueous solution and at ionic strength 0.10 M in KCl. The results revealed unusual protonation behavior, namely a surprisingly low fourth protonation constant contrary to what was expected for the compound. ^{1}H NMR and DOSY experiments, as well as molecular modeling studies, showed that the water encapsulation and the conformation observed in the solid state are retained in solution. The strong binding of the encapsulated water molecule, reinforced by the cooperative occurrence of a trifurcated hydrogen bond at the polyether compartment of the macrobicycle, account for the very low log K_4^H value obtained.

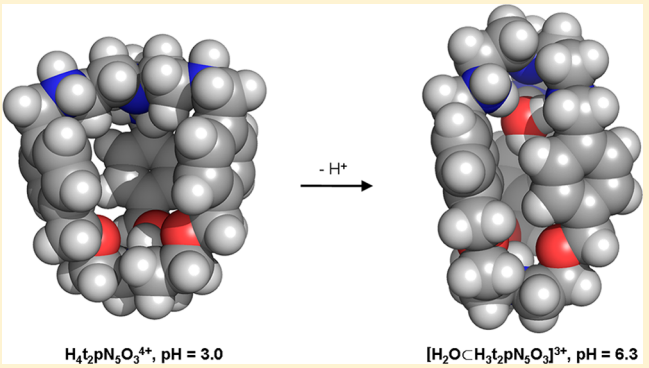

INTRODUCTION

In the biological sciences it is widely recognized that the water−protein interactions are not only fundamental in folding, conformational stability and internal dynamics of proteins, but are also important as modulators of recognition, assembling and catalysis.[1] In fact, the role of buried water molecules in protein stability and function is difficult to estimate experimentally,[2] consequently it is useful to resort to model systems to investigate the modulation of physicochemical properties of host molecules by included water.

However the role played by the water in molecular recognition by synthetic receptors is often overlooked and it is rarely seen as an active player. In the very few examples where water binding was investigated, it was observed that encapsulation of water by nitrogen based receptors leads to abnormal protonation behavior.[3] Lehn et al. reported that in a tetraoxatetraaza spheroidal macrotricyclic compound (L^1, Chart 1) the second protonation is as easy as the first one (log $K_1^H \approx$ log K_2^H = 10.5) whereas the third one is only possible at much lower pH values (log K_3^H = 5.3). This result led to the formulation of the diprotonated species as a water cryptate, the water molecule being held in an ideal tetrahedral array of hydrogen bonds, accepting two hydrogen bonds from the ammonium sites and donating two hydrogen bonds to the amine sites.[3a] Reinhoudt et al. reported a study on the acidity and water binding properties of 2,6-pyrido crown ethers of varied ring sizes (18 to 24-membered rings). In the case of the 18-membered macrocycle (L^2, Chart 1) the protonation constant of the pyridine nitrogen (log K_1^H = 4.95) is 1.59 log units to higher than that of 2,6-bis(methoxymethyl)pyridine, its noncyclic analogue, which was attributed to a stabilization of the protonated species by the presence of a water molecule accepting a hydrogen bond from the pyridinium group and donating two hydrogen bonds to ether oxygen atoms, as evidenced by X-ray crystal structures.[3b] Bharadwaj et al. reported that a small polyoxapolyaza macrobicyclic compound (L^3, Chart 1) behaves in the same way as Lehn's macrotricyclic one: the first two protonation constants are of the same

Chart 1. Compounds Used Previously in Water Binding Studies

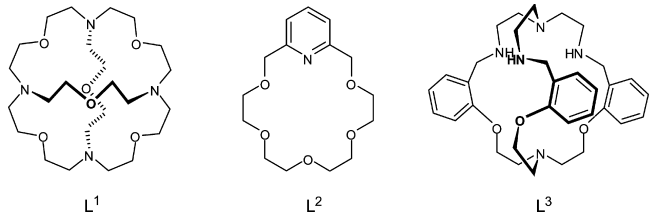

Received: April 19, 2012
Published: July 26, 2012

   dx.doi.org/10.1021/jo300799s | J. Org. Chem. 2012, 77, 6816−6824

Scheme 1. Synthetic Procedure of $t_2pN_5O_3$

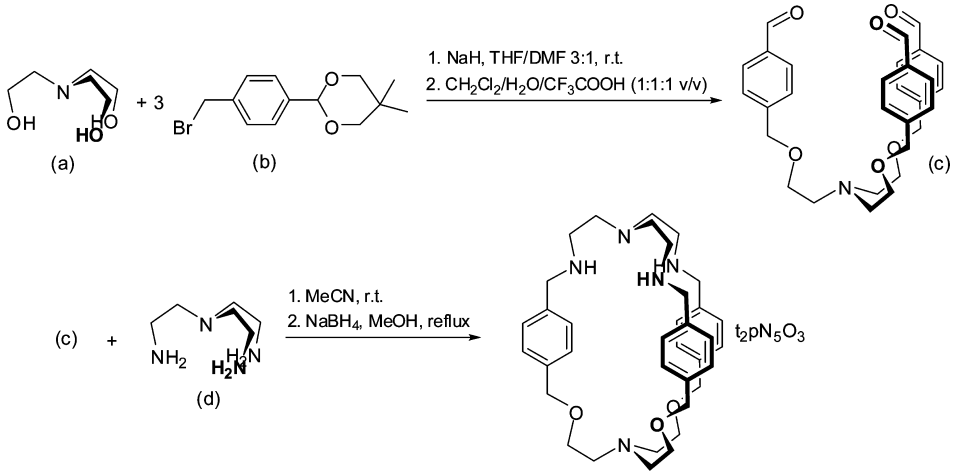

magnitude ($\log K_1^H \approx \log K_2^H = 10.45$) and the third one is much lower ($\log K_3^H = 5.56$). This result was also attributed to the presence of an encapsulated water molecule. A crystal structure also showed the water molecule held in a tetrahedral array of hydrogen bonds, accepting two hydrogen bonds from the ammonium sites and donating two hydrogen bonds to the amine sites.[3d]

Clearly, macrocyclic and macropolycyclic compounds can be useful as model systems to investigate the interaction of water molecules with host compounds and how it affects their properties. Macrobicyclic compounds in particular possess well-defined and preorganized three-dimensional cavities, able to encapsulate a wide range of cationic,[4] anionic[5] and neutral substrates.[6] Many reported crystal structures of macrobicyclic compounds show individual water molecules and even water clusters occupying molecular cavities,[3d,7] as well as mediating hydrogen bonding interactions between receptors and substrates,[8] however little is known on how water affects the conformation and chemical properties of this class of compounds in solution.

Herein is described a new heteroditopic polyoxapolyaza macrobicyclic compound whose conformation and protonation properties are shown to be dramatically influenced by an encapsulated water molecule.

RESULTS AND DISCUSSION

Synthesis of the cryptand. The synthesis of heteroditopic macrobicyclic compounds requires two critical steps: formation of a tripodal intermediate and macrobicyclization through a [1 + 1] "tripod−tripod coupling" strategy.[9] This synthetic strategy requires a bifunctional building block in which one of the functionalities is used to react in the tripodal formation reaction and the other in the macrobicyclization step.

Bharadwaj et al. have used 2-hydroxybenzaldehyde or 3-hydroxybenzaldehyde as the bifunctional building blocks in the preparation of polyoxapolyaza heteroditopic macrobicyclic compounds, which after reaction with tris(2-chloroethyl)amine in alcoholic solvents yielded the tripodal intermediate.[10]

We were interested in enlarging the cavity of such compounds by using a *p*-xylyl spacer. However an attempt to use 4-(hydroxymethyl)benzaldehyde as the bifunctional reagent and reaction with tris(2-chloroethyl)amine using the same conditions described by Bharadwaj et al., failed due to the lower nucleophilicity of the benzyl alcohol when compared with the phenyl alcohols used by those authors. Alternatively, 2-(4-bromomethyl-phenyl)-5,5-dimethyl-[1,3]dioxane (**b**) was successfully reacted with triethanolamine (**a**) to prepare the tripodal intermediate (Scheme 1). After deprotection of the aldehyde groups, the trialdehyde tripodal intermediate (**c**) was obtained for subsequent reaction with tren in a Schiff-base condensation cyclization step, which afforded $t_2pN_5O_3$ in 60% yield after imine reduction with sodium borohydride.

Crystallographic Studies. Single-crystal X-ray diffraction analysis reveals that $t_2pN_5O_3$ crystallizes from an asymmetric unit composed of one $[(H_3t_2pN_5O_3)(H_2O)]^{3+}$ cation, seven water molecules, one of them disordered over two positions (see below), and three chloride counterions, which is consistent with the molecular formula $[(H_3t_2pN_5O_3)(H_2O)]Cl_3{\cdot}7H_2O$. Furthermore, the positions of N−H hydrogen atoms were unequivocally located from the last calculated difference Fourier maps showing that two secondary amines of the tren moiety and the tertiary amine of the tripodal polyether subunit of $H_3t_2pN_5O_3^{3+}$ are protonated. One water molecule is encapsulated into the cryptand cavity establishing, as shown in Figure 1, two N−H···O hydrogen bonds with both protonated secondary amines at N···O distances of 2.751(2) and 2.773(2) Å and corresponding angles of 174(3) and 171(2)°, respectively. This water molecule is also tightly O−H···N hydrogen bonded to the third secondary amine from the tren moiety at an N···O distance of 2.597(2) Å and an angle O−H···N of 173(2)°. The proton of the tripodal nitrogen is sited from the three oxygen atoms of the polyether subunit at H···O short distances of 2.34, 2.34, and 2.38 Å, which are consistent with the existence of a trifurcated hydrogen bond with the proton encapsulated in a tetrahedral environment, as reported for TEA.[11] Three N−H binding sites from the tren moiety, pointing to the outside of the cryptand cavity, establish independent hydrogen bonds with two chloride counterions [N···Cl = 3.161(2) and 3.380(2) Å and N−H···Cl angles of 171(2) and 173(2)°, respectively] and with one crystallization water [N···O of 2.871(3) Å and O−H···N of 153(2)°]. In fact, the crystallization water molecules and chloride counterions are involved in the formation of two-dimensional network of O−H···Cl and O−H···O bonding interactions with hydrogen bond parameters listed in Table S1 (Supporting Information).

Potentiometric Studies. The protonation constants of $t_2pN_5O_3$ were determined by potentiometry in aqueous solution at 298.2 K and ionic strength 0.10 M in KCl. Two

dx.doi.org/10.1021/jo300799s | J. Org. Chem. 2012, 77, 6816−6824

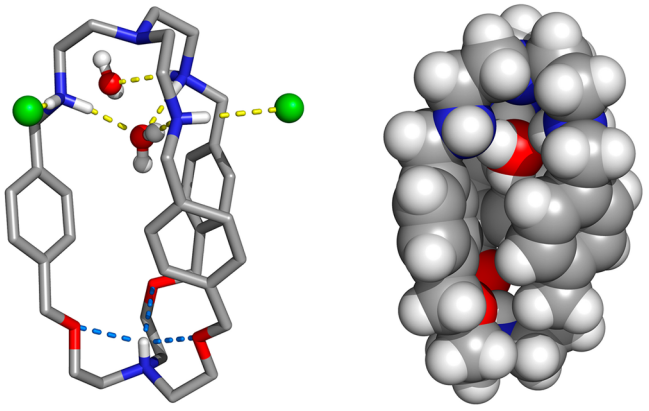

(a) (b)

Figure 1. Perspective views of $[H_3t_2pN_5O_3^{3+}\subset H_2O]$ showing different structural features of the inclusion compound: (a) view showing the encapsulated water molecule and the proton at the tripodal nitrogen involved in three hydrogen-bond interactions with $H_3t_2pN_5O_3^{3+}$; (b) space-filling model showing the water molecule encapsulated into the cryptand cage. Carbon, nitrogen, hydrogen, oxygen, and chlorine atoms are shown in gray, blue, white, red, and green, respectively. The hydrogen-bonding interactions to the tripodal proton are drawn as light blue dashed lines and the remaining ones as yellow dashed lines.

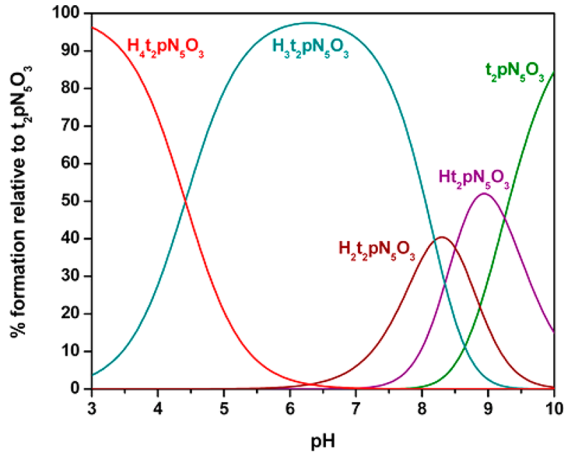

Figure 2. Species distribution diagram of the protonation of $t_2pN_5O_3$ (b). $C_{t2pN5O3} = 1.0 \times 10^{-3}$ M. Charges were omitted for clarity.

tripodal compounds, representing the polyamine and polyether compartments of $t_2pN_5O_3$, tbN_4, and TEA, respectively (Chart 2), were also studied under the same experimental conditions

Chart 2. Compounds Studied in This Work

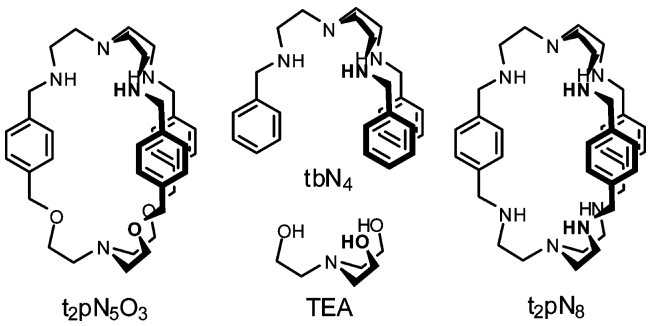

for comparison purposes. The results are collected in Table 1, the corresponding species distribution diagram are represented in Figure 2, and the titration curves are presented in the Supporting Information (Figures S1−S4).

Four protonated species of $t_2pN_5O_3$ were found in the working pH range, corresponding to the protonation of three secondary amines and a tertiary one.[12] The tertiary amine of the tren subunit can only be protonated at very low pH values due to electrostatic repulsions.[5c] Interesting to note is the fact that the protonation constants of $t_2pN_5O_3$ do not correspond to a combination of those of tbN_4 and TEA (see Table 1). The first two protonation constants of $t_2pN_5O_3$ can be unambiguously attributed to the protonation of two secondary amines (see the confirmation of the sequence of protonation in the NMR studies, below), and the values are in excellent agreement with the first two protonation constants of tbN_4. The third and fourth protonation constants, however, are quite different from the expected values, taking into account the protonation constant of TEA and the third protonation constant of tbN_4.

The third protonation constant of $t_2pN_5O_3$ could, in principle, correspond to the protonation of either the tertiary amine of the polyether subunit or the third secondary amine of the tren subunit, as the protonation constant of the third secondary amine of tbN_4 is 7.03 (in log units) and that of the tertiary amine of TEA 7.80 log units (see Table 1). The value of the fourth protonation constant is 4.41 (in log units), which is surprisingly lower than expected. This low value cannot be only explained by electrostatic repulsions within the cryptand cavity, since many polyaza cryptands of comparable size are known to be hexaprotonated at pH values of about 6,[5c] as is the case of t_2pN_8, Chart 1. The protonation constants of t_2pN_8, also determined at 298.2 K and ionic strength 0.10 M in KCl (see Table 1), have similar magnitude in pairs, as they correspond to protonation of amine centers at alternating positions in the macrobicyclic backbone, far from each other, and therefore the difference in values for each pair are mainly due to statistical

Table 1. Stepwise Protonation (K_i^H) Constants of $t_2pN_5O_3$, tbN_4, TEA, and t_2pN_8 in Aqueous Solution[a]

	log K_i^{H}[b,c]			
equilibrium reaction	$t_2pN_5O_3$	tbN_4	TEA	t_2pN_8
$L + H^+ \rightleftharpoons HL^+$	9.25(1); [9.21(2)]	9.22(1)	7.80(1)	9.18(1)
$HL^+ + H^+ \rightleftharpoons H_2L^{2+}$	8.50(1); [8.62(2)]	8.43(1)		9.03(1)
$H_2L^{2+} + H^+ \rightleftharpoons H_3L^{3+}$	8.18(1); [8.07(2)]	7.03(1)		7.76(1)
$H_3L^{3+} + H^+ \rightleftharpoons H_4L^{4+}$	4.41(1); [4.74(2)]	1.56(2)		7.35(1)
$H_4L^{4+} + H^+ \rightleftharpoons H_5L^{5+}$				6.37(1)
$H_5L^{5+} + H^+ \rightleftharpoons H_6L^{6+}$				5.73(1)

[a] $T = (298.2 \pm 0.1)$ K; $I = (0.10 \pm 0.01)$ M in KCl. [b] Values in parentheses are standard deviations in the last significant figures. [c] Values in brackets are log K_i^H values obtained after conversion of the log K_i^D determined in D_2O from ^1H NMR titration; see NMR titration below.

dx.doi.org/10.1021/jo300799s | J. Org. Chem. 2012, 77, 6816−6824

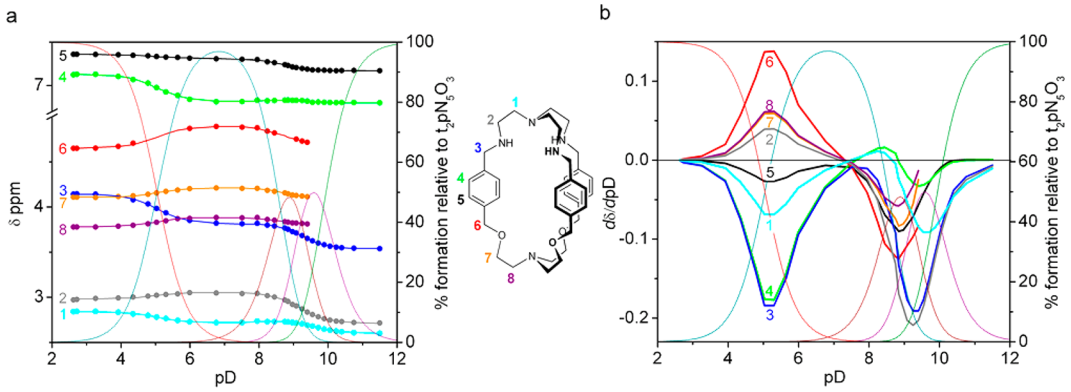

Figure 3. Titration of $H_4t_2pN_5O_3^{4+}$ in D_2O with KOD followed by ^1H NMR at 298.2 K. (a) Experimental chemical shifts as a function of pD: The solid lines are drawn by joining calculated values, obtained using the refined equilibrium constants and the individual chemical shifts. (b) First derivative of the calculated chemical shifts. Both these diagrams were drawn over the corresponding speciation diagram.

factors. Therefore, no abnormal protonation behavior was found in t_2pN_8.

The crystal structure of $[(H_3t_2pN_5O_3)(H_2O)]^{3+}$ (Figure 1) suggests that the fourth protonation occurs at a secondary amine and that its unusual low log K_4^H value is the result of the enclosed water molecule, which is so tightly bound that the protonation of the amine involved in the O−H···N hydrogen bond is highly disfavored. In addition, the trifurcated hydrogen bond taking place at the polyether compartment should contribute to stabilize a conformation of the macrobicycle, which reinforces the tight binding of the encapsulated water molecule. Indeed, it is very likely that the protonation of the tertiary amine of the polyether compartment and consequent trifurcated hydrogen bond formation preorganizes the macrobicycle in such way that binding of water is easier than a binding of another proton. Comparison of the protonation constants of $t_2pN_5O_3$ with those of L^1 and L^3 (Chart 1) confirms this point of view. In L^1 and L^3, the second protonation constant is unusually high and of the same value of the first, whereas the third is abnormally low, which means that the diprotonated species is highly stabilized by the presence of a water molecule.[3a,c] In both cases, this is due to the small size of the cavities and the ideal tetrahedral array of hydrogen bonds, in which the water molecule accepts two hydrogen bonds from the ammonium sites and donates two hydrogen bonds to the amine sites. The case of $t_2pN_5O_3$ is different: the first two protonation constants have normal values for tren-derived secondary amines (for instance, they are identical to those of model compound tbN_4, see Table 1), which means that in this case the diprotonated species is not particularly stabilized and no water molecule is bound at this stage. It is only when the tertiary amine of the polyether compartment is protonated that a water molecule is bound and has the effect of lowering the log K_4^H of $t_2pN_5O_3$. It should also be noted that the log K_3^H of $t_2pN_5O_3$ (which corresponds to the protonation of the tertiary amine of the polyether compartment) is higher than that of model compound TEA, which suggests that water binding and the formation of the trifurcated hydrogen bond occurs in a cooperative manner.

Assuming that in the absence of an encapsulated water molecule the log K_4^H of $t_2pN_5O_3$ would have the same value as the log K_3^H of tbN_4 (see Table 1), it is possible to estimate that the association constant of the included H_2O molecule is around 2.60 log units, which is a high value for the binding of a neutral molecule in highly polar medium.

NMR and Theoretical Studies. In order to confirm the protonation sequence in solution, the titration of $t_2pN_5O_3$ was followed by ^1H NMR in D_2O, at 298.2 K (see Figure 3a and Figure S5 in the Supporting Information).

As pD decreases from 12.0, resonances 1, 2, 3, and 4, corresponding to protons on the polyamine compartment, shift downfield, as expected for resonances nearby secondary amines being protonated. In the 9.5−8.0 pD region, resonances 5, 6, 7, and 8, corresponding to protons in the polyether subunit, shift downfield due to the protonation of the tertiary amine. Consequently these results confirm that the third protonation occurs at the tertiary amine, as anticipated by the determined crystal structure. As the pD drops from 6.0 to 2.5, the protonation of the third secondary amine takes place, as evidenced by the downfield shift of resonances 1, 3, and 4. After conversion of the log K_i^D determined from this titration to log K_i^H,[13] it was found that both sets of values are in very good agreement (see Table 1).

The ^1H NMR titration also provided very important structural information. For instance, it was found that resonance of protons 2 shift slightly upfield in the 6.0 to 2.5 pD region, instead of the expected downfield shift, which in addition should be of the same magnitude as resonance of protons 3 (Figure 3b). This suggests that a conformational rearrangement takes place in which protons 2 are positioned within the shielding region created by the *p*-xylyl ring, as further evidenced by the appearance of a cross peak correlating resonances of protons 2 and 4 in a NOESY spectrum recorded at pD 2.4, absent in the NOESY spectrum recorded at pD 6.8 (Figures S6 and S7 in the Supporting Information). Resonances of protons 6−8 are also shifted upfield in the 6.0−2.5 pD region (Figure 3b). As no protonation takes place near protons 6−8, the upfield shift of the corresponding resonances must also be due to the conformational rearrangement that should cause the benzene rings to change orientation in such a way that protons 6−8 become shielded. This is also in agreement with the fact that resonance 6, the closest proton to the benzene ring, is the most shifted.

The change in the value of the vicinal $^1H-^1H$ coupling constants of the protons of the ethylenic groups in the compound at the 2.5−6.0 pD region (Figure 4) gave further evidence of the conformational rearrangement. As shown in Figure 4, at pD 2.4, the resonances of protons 1 and 2 look essentially like perfect triplets, because $^3J_{AB} \approx {}^3J_{AB'} = 6.8$ Hz. This happens when the populations of the *anti* and *gauche*

dx.doi.org/10.1021/jo300799s | J. Org. Chem. 2012, 77, 6816−6824

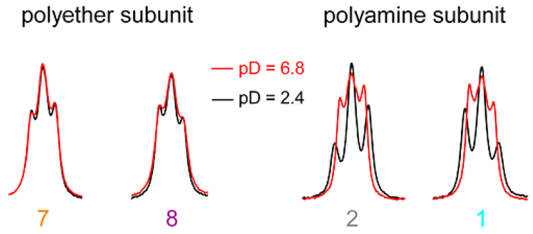

Figure 4. AA′BB′ splitting patterns of the ethylenic protons of the compound recorded at pD 6.8 and 2.4 at 298.2 K in a 400 MHz spectrometer.

conformations are close to statistical values (33% *anti*; 67% *gauche*) as a consequence of unconstrained rotation of the XCH_2-CH_2Y bond. At pD 6.8, $^3J_{AB}$ and $^3J_{AB'}$ are no longer equal as seen by the different AA′BB′ splitting pattern ($^3J_{AB}$ = 6.7 Hz and $^3J_{AB'}$ = 3.2 Hz), which is in agreement with an increase of the population of the *gauche* conformations and a more restricted rotation of the XCH_2-CH_2Y bond, consistent with the encapsulation of a water molecule, as seen in the crystal structure. Spectra recorded in the 278.2−328.2 K temperature range and at pD = 6.8 (see Figure S8 in the Supporting Information) showed that, although the rotation of the XCH_2-CH_2Y bond have increased with the temperature, the free rotation is not achieved even at the highest temperature recorded.

The $^3J_{AB}$ and $^3J_{AB'}$ of the protons of the ethylenic groups of the polyether compartment are different ($^3J_{AB}$ = 6.1 Hz and $^3J_{AB'}$ = 3.6 Hz), which indicates a preference for the *gauche* conformers. Interestingly, the AA′BB′ splitting pattern of resonances of protons 7 and 8 is the same at both pD values which means that the conformation rearrangement of the compound does not affect the population distribution of the rotamers of the polyether subunit. This is in agreement with the trifurcated hydrogen bonding taking place at the polyether compartment which should increase the preference for the *gauche* rotamers at both pD values.

In order to provide further evidence of the conformational rearrangement, diffusion ordered spectroscopy (DOSY) NMR experiments were performed with samples of $t_2pN_5O_3$ at pD = 2.4 and 6.8. DOSY experiments allow the measurement of the diffusion coefficient of a given molecular species that relates directly to its hydrodynamic radius according to the Stokes−Einstein equation.[14] It has been shown that this technique provides a way of determining small conformational or shape changes in molecular and supramolecular systems.[15]

A recent study using the same NMR instrument[16] illustrated that log D_t measurements could be measured with high precision for concentrated samples (greater than 1 mM). A change from log D_t = −9.394 at pD 2.4 to log D_t = −9.368 at pD 6.8 (+0.026 ± 0.003 log units) was determined for samples with chloride as the counterion.

The DOSY data clearly indicate that the diffusion properties of $t_2pN_5O_3$ are pH-dependent. The faster diffusion at higher pH indicates a smaller hydrodynamic radius, which is best explained by a more compact shape. We measured a sample of $t_2pN_5O_3$ with the much bulkier TsO^- counterion at pD 2.4 to discriminate between shape changes related to the tightly bound water molecule observed by other methods, and the possibility of counterion association at low pD. The diffusion coefficient for the TsO^- sample at pD 1.96 is log D_t = −9.402. This is slightly slower than the Cl^- sample, but the difference of −0.008 ± 0.003 log units is equivalent to about 30 Da and much smaller than expected from the increased molecular mass of the TsO^- complex compared to a Cl^- complex (791 Da versus 637 Da). Therefore, we conclude that $t_2pN_5O_3$ forms a compact structure at pH 6.8 that is consistent with an organized cavity and tightly bound water molecule. This is supported by molecular dynamics simulations of the tri- and tetraprotonated species of $t_2pN_5O_3$, whose distributions of radius of gyration (Figure 5) correspond to an average increase of 5% with pH

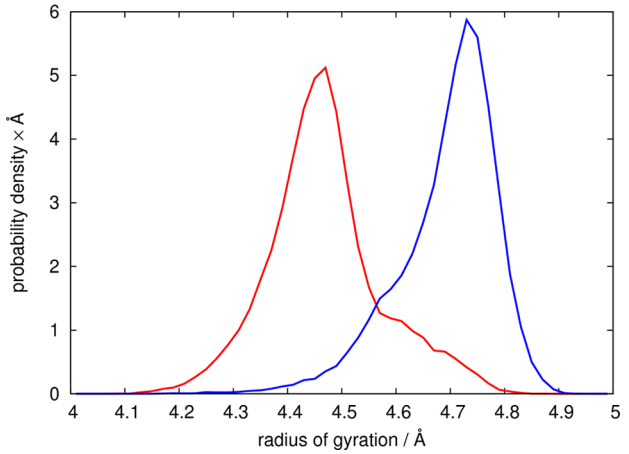

Figure 5. Distributions of the radius of gyration for $H_3t_2pN_5O_3^{3+}$ (red) and $H_4t_2pN_5O_3^{4+}$ (blue), obtained from molecular dynamics simulations.

decrease, in agreement with the 6% increase of hydrodynamic radius indicated by the diffusion coefficients reported above; the radius of gyration is the mass-weighted root-mean-square atomic distance from the center of mass and is usually proportional to the hydrodynamic radius,[17] so that their relative changes should be similar.

These data suggest that at low pH the XCH_2-CH_2Y bonds of the polyamine compartment rotate unconstrained while at higher pH such rotation is hindered because of the presence of an encapsulated water molecule, as depicted in Figure 6.

■ CONCLUSION

A new heteroditopic polyoxapolyaza macrobicyclic compound was synthesized in good yield through a [1 + 1] "tripod−tripod coupling" strategy.

The X-ray crystal structure of $H_3t_2pN_5O_3^{3+}$ revealed an encapsulated water molecule strongly bound by accepting two hydrogen bonds from two protonated secondary amines and donating a hydrogen bond to an amino group. On the other hand, the study of the acid−base properties of $t_2pN_5O_3$ showed an unusual protonation behavior, namely a value of 4.41 log units for the forth protonation constant, which is surprisingly lower than the expected one, and that cannot be explained by electrostatic repulsions within the cryptand cavity alone. Structural information in aqueous solution provided by NMR experiments showed that rotation of the XCH_2-CH_2Y bonds of the polyamine compartment of $H_3t_2pN_5O_3^{3+}$ is hindered, suggesting also the presence of one encapsulated water molecule. DOSY experiments indicated a decrease in hydrodynamic radius at higher pD, which was also supported by molecular dynamics simulations, which is consistent with a more compact molecular shape.

All these results suggest that the fourth protonation occurs at a secondary amine and that its unusual low log K_4^H value is the

dx.doi.org/10.1021/jo300799s | J. Org. Chem. 2012, 77, 6816−6824

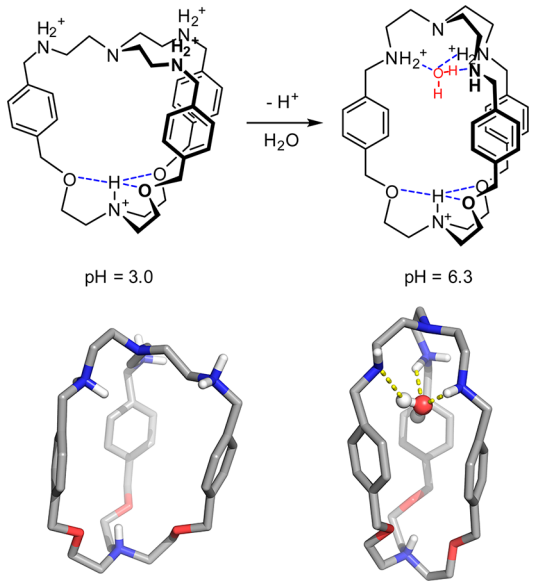

Figure 6. Proposed conformation rearrangements of $t_2pN_5O_3$ shown in schematic representation (top) and with two representative conformers from the molecular dynamics simulations (bottom).

result of the enclosed water molecule, which is so tightly bound that the protonation of the amine involved in the O−H···N hydrogen bond is highly disfavored. In addition, the trifurcated hydrogen bond taking place at the polyether compartment should contribute to stabilize a conformation of the macrobicycle, which reinforces the tight binding of the encapsulated water molecule. Indeed, the trifurcated hydrogen bond formation preorganizes the macrobicycle in such way that the binding of water is easier than a binding of another proton. The estimated association constant of the included H_2O molecule is around 2.60 log units, which is a high value for the binding of a neutral molecule in highly polar medium.

In conclusion, a large set of experiments performed in aqueous solution, using methods so different as potentiometric measurements, NMR titration, NOESY and DOSY, and molecular dynamics, point for the presence of a water molecule encapsulated into the cavity of $H_3t_2pN_5O_3^{3+}$ forming the $[H_3t_2pN_5O_3^{3+}\subset H_2O]$ entity in agreement with the single-crystal X-ray structure determination.

EXPERIMENTAL SECTION

General Considerations. All solvents and chemicals were commercially purchased reagent grade quality and used as supplied without further purification, except for triethanolamine hydrochloride, which was recrystallized from ethanol. The tbN_4, t_2pN_8 (4-diethoxymethylphenyl)methanol, and 1,3,5-tris(bromomethyl)-2,4,6-triethylbenzene compounds were prepared according to literature methods.[18−21] NMR spectra used for characterization of products were recorded on a 400 MHz instrument. NMR spectra used in the ^{1}H NMR titration were recorded on a 300 MHz instrument. The DOSY experiments were carried out in a 500 MHz instrument. TMS was used as reference for the ^{1}H NMR measurements in $CDCl_3$ and in D_2O the 3-(trimethylsilyl)propanoic acid-d_4-sodium salt. Peak assignments are based on peak integration and multiplicity for 1D ^{1}H spectra and on 2D COSY, NOESY and HMQC experiments (Figures S9−S19 in the Supporting Information).

Syntheses. *4-(Bromomethyl)benzaldehyde.* A mixture of (4-diethoxymethylphenyl)methanol (2.447 g, 11.6 mmol) and HBr 65% (65 mL) was refluxed for 1 h. The solution was cooled to rt and extracted with CH_2Cl_2 (100 mL). The organic phase was washed with a saturated solution of $NaHCO_3$, dried over anhydrous sodium sulfate, filtered, and evaporated to dryness, yielding 4-(bromomethyl)-benzaldehyde (2.190 g, 95%) which was used without purification in the next step: ^{1}H NMR (400 MHz; $CDCl_3$) δ 4.45 (s, 2H, BrCH_2*p*-xylyl), 7.49 (d, 2H, J = 8.0 Hz, *H2/H6* of *p*-xylyl), 7.80 (2H, d, J = 8.0 Hz, *H3/H5* of *p*-xylyl) and 9.95 (1H, s, *H*C═O) ppm; ^{13}C NMR (100 MHz; $CDCl_3$) δ 32.1 (BrCH_2*p*-xylyl), 129.8 (C2/*C6* of *p*-xylyl), 130.3 (*C3/C5* of *p*-xylyl), 136.3 (*C4* of *p*-xylyl), 144.4 (*C1* of *p*-xylyl), 191.6 (*C*═O) ppm.

*2-(4-Bromomethylphenyl)-5,5-dimethyl[1,3]dioxane (**b**, Scheme 1).* A mixture containing 4-(bromomethyl)benzaldehyde (2.190 g, 11 mmol), 2,2-dimethyl-1,3-propanediol (2.293 g, 22 mmol), and toluenesulfonic acid (7 mg) in toluene (13 mL) was heated to reflux for 4 h, and the azeotrope of water was received in a Dean−Stark trap. The solution was allowed to cool to rt, and the solvent was evaporated to dryness. The compound was purified by dry column vacuum chromatography using *n*-hexane/ethyl acetate (9:1) as eluent to yield the desired compound (2.767 g, 88%): ^{1}H NMR (400 MHz; $CDCl_3$) δ 0.73 (s, 3H, CH_3), 1.21 (s, 3H, CH_3), 3.58 (d, 2H, J = 12.0 Hz, CH_2), 3.70 (d, 2H, J = 12.0 Hz, CH_2), 4.41 (s, 2H, BrCH_2*p*-xylyl), 5.31 (s, 1H, C*H*), 7.32 (d, 2H, J = 8.0 Hz, *H2/H6* of *p*-xylyl), 7.41 (d, 2H, J = 8.0 Hz, *H3/H5* of *p*-xylyl) ppm; ^{13}C NMR (100 MHz; $CDCl_3$) δ 22.0 (CH_3), 23.2 (CH_3), 30.4 ($C(CH_3)_2$), 33.3 (BrCH_2*p*-xylyl), 77.8 (OCH_2), 101.4 (CH), 126.8 (*C3/C5* of *p*-xylyl), 129.2 (*C2/C6* of *p*-xylyl), 138.5 (*C1* of *p*-xylyl), 138.9 (*C4* of *p*-xylyl).

*Tripodal Trialdehyde (**c**, Scheme 1).* To a solution of triethanolamine (388 mg, 2.6 mmol) in dry THF (8 mL) was added NaH (60% dispersion in oil) (312 mg, 7.8 mmol) under nitrogen. When bubbling ceased, 2-(4-bromomethylphenyl)-5,5-dimethyl[1,3]dioxane (2.280 g, 8.0 mmol) dissolved in dry THF/DMF 3:1 mixture (32 mL) was added during 30 min. The solution was allowed to stir for 24 h and then poured into water (100 mL) and extracted with CH_2Cl_2 (3 × 100 mL). The organic portions were washed with water (3 × 100 mL) and brine (100 mL), collected in an Erlenmeyer flask, dried over anhydrous sodium sulfate, filtered, and evaporated to dryness. The solid was dissolved in CH_2Cl_2 (100 mL) to which water (100 mL) and CF_3COOH 99% (100 mL) were added. The mixture was allowed to stir for three days at 40 °C. The mixture was transferred to a separating funnel, and the aqueous phase was rejected. The organic portion was then washed with $NaHCO_3$ saturated solution (3 × 100 mL), dried over anhydrous sodium sulfate, filtered, and evaporated to dryness to give the tripodal trialdehyde (**c**) (1.178 g, 90%) which was used without purification in the next step. ^{1}H NMR (400 MHz; $CDCl_3$): δ 2.83 (t, 6H, J = 5.9 Hz, NCH_2CH_2O), 3.54 (t, 6H, J = 5.9 Hz, NCH_2CH_2O), 4.51 (s, 6H, CH_2*p*-xylyl), 7.40 (d, 6H, J = 7.9 Hz, *H2/H6* of *p*-xylyl), 7.76 (d, 6H, J = 7.9 Hz, *H3/H5* of *p*-xylyl) and 9.92 (s, 3H, *H*C═O) ppm; ^{13}C NMR (100 MHz; $CDCl_3$) δ 54.9 (NCH_2CH_2O), 69.6 (NCH_2CH_2O), 77.6 (OCH_2*p*-xylyl), 127.7 (C2/*C6* of *p*-xylyl), 130.0 (*C3/C5* of *p*-xylyl), 135.9 (*C4* of *p*-xylyl), 145.7 (*C1* of *p*-xylyl), 192.0 (C═O) ppm.

$t_2pN_5O_3$. A solution of tren (220 mg, 1.5 mmol) in MeCN (60 mL) was added dropwise over 20 min to a magnetically stirred solution of the tripodal trialdehyde (**c**) (758 mg, 1.5 mmol) in MeCN (200 mL). The mixture was allowed to stir overnight. The solvent was evaporated to dryness, the product was redissolved in MeOH (80 mL), and solid $NaBH_4$ (1.7 g, 45 mmol) was added in small portions. After the addition was completed, the mixture was allowed to stir at rt for 2 h and under reflux overnight. The solution was allowed to cool to rt, filtered, and evaporated under vacuum almost to dryness, water (20 mL) was added, and the entire methanol was evaporated. The solution was made strongly basic with 6 M KOH and extracted with $CHCl_3$ (3 × 50 mL). The organic portions were collected in an Erlenmeyer flask, dried over anhydrous sodium sulfate, filtered, and evaporated to dryness. The crude product was recrystallized from *n*-hexane to give pure $t_2pN_5O_3$ (535 mg, 60%) as a white solid: mp 116−117 °C; ^{1}H NMR (400 MHz; $CDCl_3$): δ 1.58 (br s, 3H, N−*H*), 2.56 (t, 6H, J = 5.0 Hz, NCH_2CH_2NH), 2.69 (t, 6H, J = 5.0 Hz, NCH_2CH_2NH), 2.71 (t, 6H, J = 5.0 Hz, NCH_2CH_2O), 3.53 (s, 6H, $NHCH_2$*p*-xylyl), 3.59 (t, 6H, J = 5.0 Hz, NCH_2CH_2O), 4.50 (s, 6H, *p*-xylylCH_2O), 6.78 (d, 6H, J = 7.6 Hz, *H3/H5* of *p*-xylyl), 7.02 (d, 6H, J = 7.6 Hz, *H2/H6* of *p*-

dx.doi.org/10.1021/jo300799s | J. Org. Chem. 2012, 77, 6816−6824

xylyl); ^{13}C NMR (100 MHz; $CDCl_3$) δ 48.1 (NCH_2CH_2O), 54.2 (NCH_2CH_2NH), 54.6 ($NHCH_2$*p*-xylyl), 55.7 (NCH_2CH_2NH), 68.7 (NCH_2CH_2O), 73.1 (*p*-xylylCH_2O), 127.6 (*C2*/*C6* of *p*-xylyl), 127.8 (*C3*/*C5* of *p*-xylyl) 137.4 (*C4* of *p*-xylyl), 139.1 (*C1* of *p*-xylyl); ESI–MS (MeOH) *m*/*z* 602.3 $[M + H]^+$. Anal. Calcd for $C_{36}H_{51}N_5O_3$: C, 71.85; H, 8.58; N, 11.64. Found: C, 71.80; H, 8.60; N, 11.73.

Crystals of $[H_3t_2pN_5O_3(H_2O)]Cl_3{\cdot}7H_2O$. The cryptand $t_2pN_5O_3$ (5.0 mg, 8.3 μmol) was dissolved in acetone (200 μL), and 37% HCl (2 μL) was added. A white precipitate was formed immediately. Water (20 μL) was added and the solution heated until it was clear, and then the mixture was allowed to slowly cool to rt. Single colorless crystals suitable for X-ray crystallographic determination were obtained overnight.

Potentiometric Measurements. *Reagents and Solutions.* All the solutions were prepared using dematerialized water. Carbonate-free solutions of the KOH titrant were prepared from a commercial ampule diluted with 1000 mL of water (freshly boiled for about 2 h and allowed to cool under nitrogen). These solutions were discarded every time carbonate concentration was about 0.5% of the total amount of base. The titrant solutions were standardized (tested by Gran's method).[22]

Equipment and Working Conditions. The equipment used was described before.[8f] The ionic strength of the experimental solutions was kept at 0.10 ± 0.01 M with KCl, and the temperature was maintained at 298.2 ± 0.1 K. Atmospheric CO_2 was excluded from the titration cell during experiments by passing purified nitrogen across the top of the experimental solution.

Measurements. The $[H^+]$ of the solutions was determined by the measurement of the electromotive force of the cell, $E = E'^\circ + Q \log [H^+] + E_j$. The term pH is defined as $-\log [H^+]$. E'°, Q, E_j, and K_w were determined by titration of a solution of known hydrogen-ion concentration at the same ionic strength, using the acid pH range of the titration. The liquid-junction potential, E_j, was found to be negligible under the experimental conditions used. The value of K_w was determined from data obtained in the alkaline range of the titration, considering E'° and Q valid for the entire pH range and found to be equal to $10^{-13.76}$ under our experimental conditions. Before and after each set of titrations, the glass electrode was calibrated as a $[H^+]$ probe by titration of 1.000×10^{-3} M standard HCl solution with standard KOH. Every measurement was carried out with 0.040 mmol of ligand in a total volume of 30 mL. The exact amount of ligand was obtained by determination of the excess of acid present in a mixture of the ligand and standard 1.0×10^{-2} M HCl by titration with standard KOH solution. Each titration curve consisted typically of one hundred points in the 3.0–11.0 pH range, with three replicates undertaken.

Calculation of Equilibrium Constants. Overall protonation constants, β_i^H, of the ligand were calculated by fitting the potentiometric data obtained for all the performed titrations in the same experimental conditions with the HYPERQUAD program.[23] The initial computations were obtained in the form of overall protonation constants, $\beta_i^H = [H_iL]/[H]^i[L]$. Differences, in log units, between the values of two consecutive constants provide the stepwise (log K) reaction constants (being $K_1^H = [H_iL]/[H_{i-1}L][H]$). The errors quoted are the standard deviations of the overall protonation constants given directly by the program for the input data, which include all the experimental points of all titration curves. The HYSS program[24] was used to calculate the concentration of equilibrium species from the calculated constants from which distribution diagrams were plotted.

NMR Studies. *^{1}H NMR Titration.* A solution of the $(H_4t_2pN_5O_3)(Cl)_4$ was prepared in D_2O (2.0×10^{-3} M) and during titration procedure the pD was adjusted by addition of CO_2-free KOD solutions with a microsiringe and measured with a pH meter instrument fitted with a combined microelectrode. The pH* was measured directly in the NMR tube after calibration of the microelectrode with commercial buffer aqueous solutions of standard pH 4.01 and 7.96. The final pD was calculated from the equation pD = pH* + (0.40 ± 0.02).[25] The ^{1}H NMR spectra were recorded on a 300 MHz instrument using 3-(trimethylsilyl)propanoic acid-d_4 sodium salt (DSC) as internal reference. Overall (deuteron) protonation constants, β_i^D, of the compound were calculated by fitting the data obtained with the HYPNMR program.[26] The chemical shifts of all the resonances present in the ^{1}H NMR spectra of $t_2pN_5O_3$ were used in the refinement calculations. A total of 29 data sets were used (each consisting in a measured pD value and eight recorded chemical shifts) corresponding to a total of 261 experimental values. The initial computations were obtained in the form of overall (deuteron) protonation constants, $\beta_i^D = [D_iL]/[D]^i[L]$. Conversion of the log K_i^D determined from this titration to log K_i^H was performed using the equation $\log K_i^D - \log K_i^H = 0.076 \log K_i^H - 0.05$.[13]

Determination of Vicinal ^{1}H–^{1}H Coupling Constants. Solutions of the $(H_4t_2pN_5O_3)(Cl)_4$ were prepared in D_2O (2.0×10^{-3} M) and the pD was adjusted to 2.40 and 6.80 by addition of DCl or KOD with pH meter instrument fitted with a combined microelectrode. The ^{1}H NMR spectra were recorded on a 400 MHz instrument. The AA′BB′ spin systems involving were simulated with the spectral analysis routine NUMMRIT[27] (including iteration) within the software SpinWorks.[28]

DOSY. Selected samples prepared in D_2O were analyzed by ^{1}H DOSY NMR spectra, recorded on a 500 MHz instrument fitted with a triple resonance probe and Great 50/10 gradient synthesizer (53.5 G/cm maximum output). The protocol followed that published according to Groves et al.[29] The ledbpgs2s pulse sequence was used with values of 200 ms for the diffusion delay (D20, big delta, Δ) and 1 ms for the bipolar diffusion gradient (p30, little delta, δ = 2 ms). A series of 32 spectra were stepped over the 2–95% gradient range and processed with Topspin 3.1 software. After processing into an 8k × 1k matrix, columns containing the projected diffusion parameters were summed to create the diffusion profiles from which the experimental diffusion coefficients were taken.

Crystallography. The single-crystal X-ray data of $[H_3t_2pN_5O_3(H_2O)]Cl_3{\cdot}7H_2O$ were collected at 150(2) K with graphite-monochromatized Mo Kα radiation (λ = 0.71073 Å). The selected crystal was positioned 35 mm from the CCD and the spots were measured with a counting time of 100 s. Data reduction including a multiscan absorption correction was carried out using the SAINT-NT software package. The structure was solved by a combination of direct methods with subsequent difference Fourier syntheses and refined by full matrix least-squares on F^2 using the SHELX-97 suite.[30] Anisotropic thermal displacements were used for all non-hydrogen atoms. The hydrogen atoms of the C–H bonds were placed at geometrical positions and refined with $U_{iso} = 1.2U_{eq}$ of the atom to which they are attached. The atomic positions of the hydrogen atoms of the amine groups and of seven crystallization water molecules were discernible from difference Fourier maps, and they were included in the structure refinement with individual isotropic thermal parameters. The eighth water molecule was found to be disordered over two positions, which were inserted in the structure refinement with refined occupancies of $1 - x$ and x, x being 0.55(1). Therefore, the hydrogen atoms of this single molecule were not considered in the last refinements of the crystal structure. Molecular diagrams were drawn with PyMOL software.[31] The crystal data and refinement details are summarized in Table S2 in the Supporting Information.

Molecular Modeling. Molecular dynamics simulations of $H_3t_2pN_5O_3^{3+}$ and $H_4t_2pN_5O_3^{4+}$ in water were performed with GROMACS 4.0.4.[32] Parameters compatible with the GROMOS96 53A6 force field[33] were obtained using the Automated Topology Builder[34] for both species of $t_2pN_5O_3$, and the SPC model was used for water.[35] The nonbonded interactions were treated using a twin-range cutoff of 8/14 Å, a neighbor lists update every 10 fs, and the reaction field method to treat long-range electrostatics with a dielectric constant of 54.[36,37] Berendsen coupling[38] was used to maintain the temperature at 300 K (temperature coupling of 0.1 ps) and pressure at 1 atm (isothermal compressibility of 4.5×10^{-5} bar^{-1} and pressure coupling of 0.5 ps). The time step was 2 fs, and all bonds were constrained with the LINCS algorithm.[39] A standard protocol was used to minimize and equilibrate the system before running the 50 ns long simulations.

dx.doi.org/10.1021/jo300799s | J. Org. Chem. 2012, 77, 6816–6824

■ ASSOCIATED CONTENT

Supporting Information

Titration curves of all studied compounds, ^{1}H NMR spectra recorded in the course of the titration of $H_4t_2pN_5O_3^{4+}$ with KOD in D_2O; NOESY spectra of $t_2pN_5O_3$ in D_2O at pD = 2.4 and 6.8; variable-temperature ^{1}H NMR spectra $t_2pN_5O_3$ in D_2O at pD = 6.8; NMR (^{1}H, ^{13}C, COSY, NOESY, and HMQC) and ESI-mass spectra of the reported compounds; table of hydrogen bonding parameters of the crystal structure; table with the crystal data and selected refinement details. This material is available free of charge via the Internet http://pubs.acs.org.

■ AUTHOR INFORMATION

Corresponding Author

*Tel: (+351) 21 446 9737. Fax: (+351) 21 441 1277. E-mail: delgado@itqb.unl.pt.

Notes

The authors declare no competing financial interest.

■ ACKNOWLEDGMENTS

We acknowledge Pedro Lamosa for fruitful discussions and M. C. Almeida for providing elemental analysis and ESI-MS data from the Elemental Analysis and Mass Spectrometry Service at ITQB. P.M. thanks the Fundação para a Ciência e a Tecnologia (FCT) for the grant (SFRH/BPD/79518/2011). We acknowledge FCT and POCI, with coparticipation of the European Regional Development Fund (FEDER), for financial support under project PTDC/QUI/67175/2006. The NMR spectrometers are part of The National NMR Network (REDE/1517/RMN/2005), supported by "Programa Operacional Ciência e Inovação (POCTI) 2010" and FCT. This work was also supported by FCT through grant no. PEst-OE/EQB/LA0004/2011.

■ REFERENCES

(1) Levy, Y.; Onuchic, J. N. *Annu. Rev. Biophys. Biomol. Struct.* **2006**, *35*, 389−415.

(2) Cappel, D.; Wahlström, R.; Brenk, R.; Sotriffer, C. A. *J. Chem. Inf. Model.* **2011**, *51*, 2581−2594.

(3) (a) Lehn, J.-M. *Pure Appl. Chem.* **1978**, *50*, 871−892. (b) Crootenhuis, P. D. J.; Uiterwijk, J. W. H. M.; Reinhoudt, D. N.; van Staveren, C. J.; Sudholter, E. J. R.; Bos, M.; van Eerden, J.; Klooster, W. T.; Kruise, L.; Harkema, S. *J. Am. Chem. Soc.* **1986**, *108*, 780−788. (c) Bazzicalupi, C.; Bandyopadhyay, P.; Bencini, A.; Bianchi, A.; Giorgi, C.; Valtancoli, B.; Bharadwaj, D.; Bharadwaj, P. K.; Butcher, R. J. *Eur. J. Inorg. Chem.* **2000**, 2111−2116. (d) Chand, D. K.; Ragunathan, K. G.; Mak, T. C. W.; Bharadwaj, P. K. *J. Org. Chem.* **1996**, *61*, 1169−1171.

(4) Zhang, X. X.; Izatt, R. M.; Bradshaw, J. S.; Krakowiak, K. E. *Coord. Chem. Rev.* **1998**, *174*, 179−189.

(5) (a) McKee, V.; Nelson, J.; Town, R. M. *Chem. Soc. Rev.* **2003**, *32*, 309−325. (b) Kang, S. O.; Hossain, M. A.; Bowman-James, K. *Coord. Chem. Rev.* **2006**, *250*, 3038−3052. (c) Mateus, P.; Bernier, N.; Delgado, R. *Coord. Chem. Rev.* **2010**, *254*, 1726−1747.

(6) Seel, C.; Vögtle, F. *Angew. Chem., Int. Ed. Engl.* **1992**, *31*, 528−549.

(7) (a) Chand, D. K.; Bharadwaj, P. K. *Inorg. Chem.* **1998**, *37*, 5050−5055. (b) Hossain, M. A.; Llinares, J. M.; Alcock, N. W.; Powell, D.; Bowman-James, K. *J. Supramol. Chem.* **2002**, *2*, 143−149. (c) Refat, M. S.; Gotoh, K.; Ishida, H. *Acta Crystallogr.* **2006**, *E62*, o4407−o4409. (d) Lakshminarayanan, P. S.; Kumar, D. K.; Ghosh, P. *Inorg. Chem.* **2005**, *44*, 7540−7546. (e) Ravikumar, I.; Lakshminarayanan, P. S.; Suresh, E.; Ghosh, P. *Cryst. Growth Des.* **2006**, *6*, 2630−2633. (f) Lakshminarayanan, P. S.; Ravikumar, I.; Suresh, E.; Ghosh, P. *Cryst. Growth Des.* **2008**, *8*, 2842−2852. (g) Li, Y.; Jiang, L.; Feng, X.-L.; Lu, T.-B. *Cryst. Growth Des.* **2008**, *8*, 3689−3694. (h) Yang, L.-Z.; Li, Y.; Jiang, L.; Feng, X.-L.; Lu, T.-B. *CrystEngComm* **2009**, *11*, 2375−2380.

(8) (a) Hynes, M. J.; Maubert, B.; McKee, V.; Town, R. M.; Nelson, J. *J. Chem. Soc., Dalton Trans.* **2000**, 2853−2859. (b) Hossain, M. A.; Llinares, J. M.; Mason, S.; Morehouse, P.; Powell, D.; Bowman-James, K. *Angew. Chem., Int. Ed.* **2002**, *41*, 2335−2338. (c) Hossain, M. A.; Morehouse, P.; Powell, D.; Bowman-James, K. *Inorg. Chem.* **2005**, *44*, 2143−2149. (d) Ravikumar, I.; Lakshminarayanan, P. S.; Suresh, E.; Ghosh, P. *Beilstein J. Org. Chem.* **2009**, *5*(41). (e) Mateus, P.; Delgado, R.; Brandão, P.; Félix, V. *J. Org. Chem.* **2009**, *74*, 8638−8646. (f) Mateus, P.; Delgado, R.; Brandão, P.; Carvalho, S.; Félix, V. *Org. Biomol. Chem.* **2009**, *7*, 4661−4637.

(9) Dietrich, B.; Hosseini, M. W.; Lehn, J.-M.; Sessions, R. B. *Helv. Chim. Acta* **1985**, *68*, 289−299.

(10) (a) Chand, D. K.; Bharadwaj, P. K. *Inorg. Chem.* **1996**, *35*, 3380−3387. (b) Ghosh, P.; Gupta, S. S.; Bharadwaj, P. K. *J. Chem. Soc., Dalton Trans.* **1997**, 935−938.

(11) Naiini, A. A.; Pinkas, J.; Plass, W.; Young, V. G., Jr.; Verkade, J. G. *Inorg. Chem.* **1994**, *33*, 2137−2141.

(12) Bencini, A.; Bianchi, A.; Garcia-España, E.; Micheloni, M.; Ramirez, J. A. *Coord. Chem. Rev.* **1999**, *188*, 97−156.

(13) Krężel, A.; Bal, W. *J. Inorg. Biochem.* **2004**, *98*, 161−166.

(14) Cohen, Y.; Avram, L.; Evan-Salem, T.; Frish, L. In *Analytical Methods in Supramolecular Chemistry*; Schalley, C., Ed.; Wiley-VCH: Weinheim, 2007; pp 163−219.

(15) Giuseppone, N.; Schmitt, J.-L.; Allouche, L.; Lehn, J.-M. *Angew. Chem., Int. Ed.* **2008**, *47*, 2235−2239.

(16) Reinstein, O.; Neves, M. A. D.; Saad, M.; Boodram, S. N.; Lombardo, S.; Beckham, S. A.; Brouwer, J.; Audette, G. F.; Groves, P.; Wilce, M. C. J.; Johnson, P. E. *Biochemistry* **2011**, *50*, 9368−9376.

(17) Teraoka, I. *Polymer Solutions*; Schalley, C., Ed.; Wiley: New York, 2002; pp 184−188.

(18) Collman, J. P.; Fu, L.; Herrmann, P. C.; Wang, Z.; Rapta, M.; Bröring, M.; Schwenninger, R.; Boitrel, B. *Angew. Chem., Int. Ed.* **1998**, *37*, 3397−3400.

(19) Lakshminarayanan, P. S.; Ravikumar, I.; Suresh, E.; Ghosh, P. *Cryst. Growth Des.* **2008**, *8*, 2842−2852.

(20) Sarri, P.; Venturi, F.; Cuda, F.; Roelens, S. *J. Org. Chem.* **2004**, *69*, 3654−3661.

(21) Wallace, K. J.; Hanes, R.; Anslyn, E. V.; Morey, J.; Kilway, K. V.; Siegel, J. *Synthesis* **2005**, 2080−2083.

(22) Rossotti, F. J.; Rossotti, H. J. *J. Chem. Educ.* **1965**, *42*, 375−378.

(23) Gans, P.; Sabatini, A.; Vacca, A. *Talanta* **1996**, *43*, 1739−1753.

(24) Alderighi, L.; Gans, P.; Ienco, A.; Peters, D.; Sabatini, A.; Vacca, A. *Coord. Chem. Rev.* **1999**, *184*, 311−318.

(25) Delgado, R.; da Silva, J. J. R. F.; Amorim, M. T. S.; Cabral, M. F.; Chaves, S.; Costa, J. *Anal. Chim. Acta* **1991**, *245*, 271−282.

(26) (a) Frassineti, C.; Ghelli, S.; Gans, P.; Sabatini, A.; Moruzzi, M. S.; Vacca, A. *Anal. Biochem.* **1995**, *231*, 374−382. (b) Frassineti, C.; Alderighi, L.; Gans, P.; Sabatini, A.; Vacca, A.; Ghelli, S. *Anal. Bioanal. Chem.* **2003**, *376*, 1041−1052.

(27) Quirt, A. R.; Martin, J. S. *J. Magn. Reson.* **1971**, *5*, 318−327.

(28) Marat, K. SpinWorks 3.1.7, University of Manitoba, Canada, 2010, http://home.cc.umanitoba.ca/~wolowiec/spinworks/index.html.

(29) Groves, P.; Rasmussen, M. O.; Molero, M. D.; Samain, E.; Canada, F. J.; Driguez, H.; Jimenez-Barbero, J. *Glycobiology* **2004**, *14*, 451−456.

(30) Sheldrick, G. M. *Acta Crystallogr.* **2008**, *A64*, 112−122.

(31) The PyMOL Molecular Graphics System, Version 1.2r3pre, Schrödinger, LLC.

(32) Hess, B.; Kutzner, C.; van der Spoel, D.; Lindahl, E. *J. Chem. Theor. Comput.* **2008**, *4*, 435−447.

(33) Oostenbrink, C.; Villa, A.; Mark, A. E.; van Gunsteren, W. F. *J. Comput. Chem.* **2004**, *25*, 1656−1676.

(34) Malde, A. K.; Zuo, L.; Breeze, M.; Stroet, M.; Poger, D.; Nair, P. C.; Oostenbrink, C.; Mark, A. E. *J. Chem. Theor. Comput.* **2011**, *7*, 4026−4037.

(35) Hermans, J.; Berendsen, H. J. C.; van Gunsteren, W. F.; Postma, J. P. M. *Biopolymers* **1984**, *23*, 1513−1518.
(36) Barker, J. A.; Watts, R. O. *Mol. Phys.* **1973**, *26*, 789−792.
(37) Smith, P. E.; van Gunsteren, W. F. J. *Chem. Phys.* **1994**, *100*, 3169−3174.
(38) Berendsen, H. J. C.; Postma, J. P. M.; van Gunsteren, W. F.; DiNola, A.; Haak, J. R. *J. Chem. Phys.* **1984**, *81*, 3684−3690.
(39) Hess, B.; Bekker, H.; Berendsen, H. J. C.; Fraaije, J. G. E. M. *J. Comput. Chem.* **1997**, *18*, 1463−1472.